Universität des Saarlandes

Fachrichtung Mathematik

Galerkin-Petrov approach for the Boltzmann equation

Irene M. Gamba and Sergej Rjasanow

Galerkin-Petrov approach for the Boltzmann equation

Irene M. Gamba

The University of Texas at Austin
Department of Mathematics
Austin, Texas 7871
USA
gamba@math.utexas.edu

Sergej Rjasanow

Saarland University
Department of Mathematics
P.O. Box 15 11 50
66041 Saarbrücken
Germany
rjasanow@num.uni-sb.de

Galerkin-Petrov approach for the Boltzmann equation

Irene M. Gamba[*]   Sergej Rjasanow[†]

August 8, 2017

Abstract

In this work, we we propose a new Galerkin-Petrov method for the numerical solution of the classical spatially homogeneous Boltzmann equation. This method is based on an approximation of the distribution function by associated Laguerre polynomials and spherical harmonics and test an a variational manner with globally defined three-dimensional polynomials. A numerical realisation of the algorithm is presented. The algorithmic developments are illustrated with the help of several numerical tests.

1   Introduction

In this paper, we propose a new Galerkin-Petrov method for the numerical solution of the classical spatially homogeneous Boltzmann equation. This method is based on an approximation of the distribution function by associated Laguerre polynomials and spherical harmonics. The test functions are polynomials defined globally in $\mathbb{R}^3$. This choice leads to a rapid numerical scheme with a high spectral accuracy for smooth solutions.

Deterministic methods for the Boltzmann equation have been extensively studied in the last decades. Overview of these methods can be found, for example, in the book of V. Aristov [2] and in a more recent review by A. Narayan and A. Klöckner [34]. Since the pioneering work of D. Goldstein, B. Sturtevant and J. E. Broadwell [24], many authors proposed different ideas on how to derive a discrete version of the Boltzmann collision operator [35],[43],[46],[41],[36],[37]. In [29] the authors studied the difference scheme for a mixture of gases. L. Pareschi and G. Russo [39],[40] considered deterministic spectral methods for the Boltzmann equation based on the Fourier transform. In our paper, we limit our consideration to a particular class of deterministic methods, namely, those based on mesh-free Galerkin-Petrov discretisation. The main difficulty within the deterministic approximation of the Boltzmann collision integral, besides its high dimensionality, is the fact that a grid for the integration over the velocity space $\mathbb{R}^3$ is not suitable for the integration over the set of all

---

[*]The University of Texas at Austin, Austin, Texas 7871, USA
[†]Saarland University, 66041 Saarbrücken, Germany

directions (i.e. the unit sphere S^2). In the case of a regular tensor discretisation of the velocity space with n points in each direction, only $\mathcal{O}(n)$ irregularly distributed integration points would belong to the unit sphere. A. Bobylev, A. Palczewski and J. Schneider [11] considered this direct approximation of the Boltzmann collision integral and showed that the corresponding numerical method is consistent. This method requires $\mathcal{O}(n^7)$ arithmetical operations per time step and has the formal accuracy of $\mathcal{O}(n^{-1/2})$. A. Bobylev and S. Rjasanow considered the case of the Maxwell pseudo-molecules and utilised an explicit simplification of the Boltzmann equation for this model of interaction alongside with the Fast Fourier Transform (FFT) to develop a deterministic numerical method [12], [13]. Their method requires $\mathcal{O}(n^4)$ arithmetical operations per time step and achieves the same low formal accuracy order of $\mathcal{O}(n^{-1/2})$. A similar method was proposed by L. Pareschi and B. Perthame in [38]. It appears to be the fastest known deterministic numerical method on an uniform grid. At the same time, its applications are strongly restricted to the case of Maxwell pseudo-molecules. Considering the case of hard spheres, A. Bobylev and S. Rjasanow [14] developed an algorithm, where the integration over the unit sphere is completely separated from the integration over the whole space $\mathbb{R}^3$. The resulting scheme utilises fast evaluation of the generalised Radon and X-Ray transforms via the FFT and requires $\mathcal{O}(n^6 \log(n))$ operations per time step with the high formal accuracy of $\mathcal{O}(n^{-2})$. A further development of this approach in [21] led to spectral schemes for more general collision kernels with a higher efficiency. I. Ibragimov and S. Rjasanow in [26] used a special form of the Boltzmann collision operator, which led to a possibility to omit numerical integration over the unit sphere. This idea was later used by I. M. Gamba and S. H. Tharkabhushanam [22], [23], to handle the granular inelastic Boltzmann equation. It was developed further in the recent paper [20] for most general collision cross-section with anisotropic angular scattering that includes grazing collisions approximating the Landau collision operator. These methods have also been extended to treat systems of Boltzmann equations for gas mixtures and multi-energy level gases (see [33], [48]). In these extensions of the scheme, the Langrange multiplier method is employed to enforce the total conservation properties associated with the mixture. The first result on error estimates and convergence to Boltzmann-Maxwell equilibrium states for Lagrangian based conservative spectral methods for the Boltzmann equation with elastic interactions and hard potential with angular cut-off collision kernels was published in [1]. A survey of this subject can be found in [19]. While the majority of authors use an uniform grid in the velocity space, in [25] A. Heintz, P, Kowalczyk and R. Grzhibovskis have used a non-uniform grid.

Reviews of an already substantial amount of publications on the Discrete Velocity Models (DVM) for the Boltzmann equation can be found in [6] and in [8]. Constructive ideas in this area have been recently proposed by H. Babowsky and his co-authors in [3],[4]. Two recent ideas regarding the deterministic solution of the Boltzmann equation are the use of the Galerkin schemes based on global basis functions (see unpublished manuscripts [18],[28]) and the approximation by means of three-dimensional algebraic tensors [27],[5]. We refer to the recent monograph by B. Shizgal [45] devoted to the spectral methods and an enormous amount of cited literature therein. The approach most similar to ours can be found in [16]. Its

realisation for a rather simple isotropic situation is published in [17].

This paper is organised as follows. In Section 2, we give a short description of an initial value problem for the Boltzmann equation and present different collision kernels. In Section 3, an abstract version of Galerkin-Petrov method for a general bilinear operator is formulated. We describe a set of basis and test functions in terms of classical polynomials and spherical harmonics. Furthermore, the mass and collision matrices are presented in all details. A numerical realisation of the algorithm is described in Section 4. Here, we use a numerical integration for the entries of the mass and collision matrices and describe possible time integration schemes. Finally, in Section 5, we present the results of numerical computations done by the new method for different initial value problems and different collision kernels. Conclusions and an outlook can be found in Section 6.

2 Boltzmann equation

We consider the initial value problem for the classical spatially homogeneous Boltzmann equation

$$\frac{\partial}{\partial t} f(t,v) = Q(f,f)(t,v), \quad t \in \mathbb{R}_+, \ v \in \mathbb{R}^3, \tag{1}$$

which describes the time evolution of the probability density

$$f \ : \ \mathbb{R}_+ \times \mathbb{R}^3 \to \mathbb{R}_+$$

from its initial value

$$f(0,v) = f_0(v)$$

to the final Maxwell distribution

$$\lim_{t \to \infty} f(t,v) = f_M(v) = \frac{\rho_0}{(2\pi \, T_0)^{3/2}} \, \mathrm{e}^{-\dfrac{|v - V_0|^2}{2 \, T_0}}. \tag{2}$$

The right-hand side of the equation (1), known as the collision integral or the collision term, has the form

$$Q(f,f)(t,v) = \int\limits_{\mathbb{R}^3} \int\limits_{S^2} B(v,w,e) \Big(f(t,v')f(t,w') - f(t,v)f(t,w) \Big) \, de \, dw. \tag{3}$$

Here $v, w \in \mathbb{R}^3$ are the post-collision velocities, $e \in S^2 \subset \mathbb{R}^3$ is a unit vector, $v', w' \in \mathbb{R}^3$ are the pre-collision velocities, and $B(v,w,e)$ is the collision kernel. The operator $Q(f,f)$ represents the change of the distribution function f due to the binary collisions between particles. A single collision results in the change of the velocities of the colliding partners

$$v', w' \ \to v, w. \tag{4}$$

The reversible or elastic collision transformation (4) conserves the momentum and the energy

$$v + w = v' + w', \quad |v|^2 + |w|^2 = |v'|^2 + |w'|^2, \tag{5}$$

3

implying that the post- and pre-collisional relative velocities $u = v - w$ and $u' = v' - w'$, respectively, have the same magnitude, i.e. $|u'| = |u|$. The renormalised pre-collisional relative velocity u' defines the scattering direction denoted by the unit vector e, namely

$$e = u'|u'|^{-1} = u'|u|^{-1}\,.$$

In particular, the conservative exchange of binary states (5) can be written in the following centre of mass - relative velocity coordinates form

$$v' = \frac{1}{2}\Big(v + w + |u|e\Big)\,, \quad w' = \frac{1}{2}\Big(v + w - |u|e\Big)\,, \quad e \in S^2\,.$$

In this frame of reference, the collision kernel, or transition probability rate from the pre to post states, is, in general, a mapping

$$B \ : \ \mathbb{R}^3 \times \mathbb{R}^3 \times S^2 \to \mathbb{R}_+. \tag{6}$$

It usually is written in a form of a product of a power function of the relative speed and a scattering angular function

$$B(v, w, e) = B\left(|u|, \frac{(u, e)}{|u|}\right) = C_\lambda\, |u|^\lambda\, b\left(\frac{(u, e)}{|u|}\right)\,, \quad -3 < \lambda \le 1\,. \tag{7}$$

These kernels include hard spheres ($\lambda = 1$ and $b = 1$), hard potentials ($0 < \lambda < 1$), Maxwell pseudo-molecules ($\lambda = 0$), and soft potentials models ($-3 < \lambda < 0$). In addition, the weak formulation associated to the Boltzmann equation can be derived using the binary structure, the conservative collision law, and the the symmetries of the collision kernel with respect to the exchange of variables (6). This weak form reads

$$\frac{\partial}{\partial t}\int\limits_{\mathbb{R}^3} f(t, v)\psi(v)\, dv = \int\limits_{\mathbb{R}^3} Q(f, f)(t, v)\psi(v)\, dv$$

$$\tag{8}$$

$$= \int\limits_{\mathbb{R}^3}\int\limits_{\mathbb{R}^3} f(t, v)f(t, w)\int\limits_{S^2} B(v, w, e)\Big(\psi(v') + \psi(w') - \psi(v) - \psi(w)\Big)\, de\, dw\, dv$$

for any test function ψ that makes this integral finite. Note that in this weak formulation $\psi(v')$ and $\psi(w')$ are the evaluations in the post-collisional velocities. This is what subtlety marks the stability of the Boltzmann equation through the H-Theorem given below. Taking $\psi \in \mathrm{span}\{1, v, |v|^2\}$ and using the elastic exchange of coordinates (5), the following conserved quantities are found

$$\frac{\partial}{\partial t}\int\limits_{\mathbb{R}^3} f(t, v)\begin{pmatrix} 1 \\ v \\ |v|^2 \end{pmatrix} dv = \int\limits_{\mathbb{R}^3} Q(f, f)(t, v)\begin{pmatrix} 1 \\ v \\ |v|^2 \end{pmatrix} dv = \begin{pmatrix} 0 \\ 0 \\ 0 \end{pmatrix}\,.$$

Thus, the functions from the set $\{1, v, |v|^2\}$ are called collision invariants.

Finally, we recall the H-theorem that can be obtained by testing with $\psi = f(t, \cdot)$. If $f \in C^1\Big((0, \infty), L^1(\mathbb{R}^3)\Big)$, then

$$\frac{\partial}{\partial t} \int_{\mathbb{R}^3} f(t, v) \ln f(t, v) \, dv = \int_{\mathbb{R}^3} Q(f, f)(t, v) \ln f(t, v) \, dv =$$

$$-\int_{\mathbb{R}^3 \times \mathbb{R}^3 \times S^2} (f(v',t) f(w',t) - f(v,t) f(w,t)) \frac{\ln(f(v',t) f(w',t))}{\ln(f(v,t) f(w,t))} B(v, w, e) de \, dw \, dv \leq 0 \,.$$

As anticipated in (2), the Boltzmann H-theorem ensures that the unique stationary equilibrium state is a Maxwell distribution, whose moments are the the same as those of the initial state. In addition, this stationary equilibrium state is stable with convergence rates depending on the potential rates λ and the integrability properties of the angular part b. We assume that the angular part b of the collision kernel is integrable over $e \in S^2$. If, in addition, the angular function b is bounded, this condition is referred as the Grad's cut-off. The integrability condition of the angular part b implies that the collision operator $Q(f, f)$ splits into a difference of two positive operators,

$$Q(f, f)(t, v) = Q^+(f, f)(t, v) - Q^-(f, f)(t, v) = Q^+(f, f)(t, v) - f(t, v) \nu(t, v),$$

where

$$Q^+(f, f)(t, v) = \int_{\mathbb{R}^3} \int_{S^2} B(v, w, e) f(t, v') f(t, w') \, de \, dw$$

is the gain operator, and

$$Q^-(f, f)(t, v) = f(t, v) \nu(t, v)$$

is the loss operator, provided that the collision frequency integral

$$\nu(t, v) = \int_{\mathbb{R}^3} \int_{S^2} B(v, w, e) f(t, w) \, de \, dw$$

is well defined. Without loss of generality, we assume

$$\frac{1}{4\pi} \int_{S^2} b\Big(\frac{(u, e)}{|u|}\Big) \, de = \frac{1}{2} \int_{-\pi}^{\pi} b(\cos\theta) \sin\theta \, d\theta = 1 \,. \tag{9}$$

It is important to point out, that the case $\lambda = -3$, corresponding to the Coulomb interaction, can not be modelled by the Boltzmann equation if the function $b(\cos\theta) = \cos((u, e)|u|^{-1})$ is integrable. This is due to the divergence of the integral of $f * |u|^{-3}$ in 3-dimensions for any integrable $f(t, \cdot)$ in v-space. The loss operator $Q^-(f, f)$ is not well defined in this case.

We will also consider the special forms of isotropic cut-off kernel B, namely the Variable Hard Spheres model (VHS), see [7]. In this model the angular dependence of the scattering is isotropic, i.e. independent of the scattering angle

$$B(v, w, e) = C_\lambda |u|^\lambda, \quad -3 < \lambda \leq 1 \,. \tag{10}$$

Our approach can be extended to treat many interesting non-cut-off collision kernels, in which the angular scattering function $b(\cos(\theta))$ becomes singular as the scattering angle θ approaches zero, or equivalently

$$\cos\theta = \frac{(u,e)}{|u|} \to 1 \,. \tag{11}$$

This limit can be associated to a singular behaviour for near grazing collisions corresponding to interactions where $v' \approx v$ and $w \approx w$. Indeed, by the conservative interaction law the relation

$$|v' - v|^2 = |w' - w|^2 = |u|^2 \, \frac{1 - \cos\theta}{2} \,, \tag{12}$$

or equivalently

$$|v' - v| = |w' - w| = |u| \sin\frac{\theta}{2}$$

holds. This implies, that $|v' - v| \approx 0$ is equivalent to $\sin(\theta/2) \approx 0$ independently on the norm of the relative speed $|u|$.

While we will not cover the non cut-off case in this study. We expect, however, that an application of our proposed Galerkin-Petrov scheme will address this case as well. It can be done along the lines of the references [47], [49], where a classical Discontinuous Galerkin, or a non-conformal Finite Element Method, was developed to compute the spectrum of the linearised Boltzmann equation for angular non cut-off scattering kernels ranging from hard to soft potentials.

The computational approach for the non cut-off case in these studies uses the weak formulation (8) with the second order Taylor expansion of the test function terms $\varphi(v') - \varphi(v)$. This makes it possible to perform the cancellation of non-integral angular singularities analytically, i.e. by means of the relation (12). Thus, a sound numerical scheme, which is able to handle proper Rayleigh quotients, is formulated. A novel way to numerically compute Rayleigh quotients for solutions of the linearised radial Landau equation by means of Laguerre polynomial expansion can be found in a recent publication [10]. This work relates to our Galerkin Method approach, since it indicates, that we can handle the spectral analysis of general, non-radial solutions of both the linearised Boltzmann and Landau equations. We will elaborate on this feature of the method in an upcoming paper.

The fast solver derived in this paper can be used to compute anisotropic collisions for grazing limits. This allows for obtaining approximation rates of the Landau operator by a sequence of Boltzmann operators, similarly as it was done in [20], where a spectral Lagrangian constrains method was employed. One starts by solving the initial value problem for the non-linear Boltzmann equation (1)-(3) in 3-dimensions in velocity space with the Coulomb interaction ($\lambda = -3$). The collision kernels are given by a 2-parameter family $(\varepsilon, \delta) \in (0,1] \times [0,2)$ of cut-off angular cross sections as

$$b_\varepsilon^\delta\Big(\frac{(u,e)}{|u|}\Big) = b_\varepsilon^\delta(\cos\theta) = -\frac{4}{2\pi H_\delta(\sin(\varepsilon/2))} \, \frac{1}{\cos^{3+\delta}\theta} \, \mathbb{1}_{\cos\theta \geq \sin(\varepsilon/2)} \,. \tag{13}$$

6

with

$$H_\delta(x) = \begin{cases} \log x, & \text{for } \delta = 0, \\ -\frac{x^{-\delta}}{\delta}, & \text{for } 0 < \delta < 2. \end{cases} \tag{14}$$

Note that the case $\delta = 0$ corresponds to the Rutherford cross section. The corresponding Landau operator limit is independent of the angular scattering cross section b_ε^δ. Omitting the time variable, it can be written as

$$Q_L(f,f)(v) = \operatorname{div}_v\left(\int_{\mathbb{R}^3} |u|^{\lambda+2}\left(I - \frac{u \otimes u}{|u|^2}\right)\left(f(w)\nabla_v f(v) - f(v)\nabla_w f(w)\right) dw\right).$$

The value $\delta = 0$ is the smallest possible exponent when it is possible to obtain the Landau equation. For any value $\delta > 2$, however, it is impossible to control the higher terms of the expansion (see [20]). This particular case will be the subject of our study an upcoming paper.

3 Galerkin-Petrov approximation

Let $\mathbb{V}$ be a space of functions with three independent variables and

$$Q : \mathbb{V} \times \mathbb{V} \to \mathbb{V} \tag{15}$$

a bilinear operator. Let

$$f : \mathbb{R}_+ \times \mathbb{R}^3 \to \mathbb{R}$$

be a time dependent function with

$$f(t,\cdot) \in \mathbb{V} \quad \text{for all } t \in \mathbb{R}_+.$$

We consider an initial value problem

$$f_t = Q(f,f), \quad \text{for } t > 0, \quad f(0,\cdot) = f_0. \tag{16}$$

By the use of a finite dimensional subspace $\mathbb{V}_n$ of the space $\mathbb{V}$ having a basis

$$\Phi = \left(\varphi_1, \ldots, \varphi_n\right), \tag{17}$$

we consider an approximation of the function f in the form

$$f^{(n)} = \Phi \underline{f} = \sum_{j=1}^n f_j \varphi_j, \quad \underline{f} \in \mathbb{R}^n. \tag{18}$$

Furthermore, let

$$\mathbb{V}_n^* \subseteq \mathbb{V}^*$$

be a finite dimensional subspace of the space $\mathbb{V}^*$ of distributions over $\mathbb{V}$ having a basis

$$\Psi = \left(\psi_1, \ldots, \psi_n\right). \tag{19}$$

7

Then the Galerkin-Petrov scheme for the equation (16) reads as follows. Find $f^{(n)}(t, \cdot) \in \mathbb{V}_n$ such that the Galerkin-Petrov equations

$$\frac{d}{dt} < f^{(n)}(t, \cdot), \psi_i > = < Q(f^{(n)}(t, \cdot), f^{(n)}(t, \cdot)), \psi_i >, \quad i = 1, \ldots, n \qquad (20)$$

with the initial condition

$$< f^{(n)}(0, \cdot), \psi_i > = < f_0, \psi_i >, \quad i = 1, \ldots, n \qquad (21)$$

are satisfied for $t > 0$. Here, the brackets $< \cdot, \cdot >$ denote the action of the distribution $\psi_i \in \mathbb{V}^*$ on a function from $\mathbb{V}$. The system (20) is in fact a system of ordinary differential equations for the time-dependent coefficients f_j of the vector $\underline{f} \in \mathbb{R}^n$. By the use of the bilinear structure of the operator Q, we get a shorter form of the system (20)

$$\frac{d}{dt} \left(M \underline{f}(t) \right)_i = \underline{f}(t)^\top Q_i \underline{f}(t), \quad i = 1, \ldots, n \qquad (22)$$

and

$$M \underline{f}(0) = \underline{f}_0, \quad \left(\underline{f}_0 \right)_i = < f_0, \psi_i >, \quad i = 1, \ldots, n.$$

The matrices Q_i have the entries of the following form

$$Q_i[k, \ell] = < Q(\varphi_k, \varphi_\ell), \psi_i >, \quad i, k, \ell = 1, \ldots, n,$$

while the mass matrix M is defined as

$$M[i, j] = < \varphi_j, \psi_i >, \quad i, j = 1, \ldots, n.$$

Turning back to the Boltzmann equation, we assume that the initial condition f_0 belongs to the Schwartz space $\mathbb{S}$ of infinitely smooth functions all of whose derivatives are rapidly decreasing. Then the solution f of the Boltzmann equation $f(t, \cdot)$ is again a Schwartz space function for all times t, see [15]. Thus, the basis functions φ_j belong to the subspace

$$\mathbb{S}_n = \text{span} \Phi \subset \mathbb{S}.$$

The dual space $\mathbb{S}^*$ is the space of tempered distributions. The space $\mathbb{S}^*$ contains among others polynomials of arbitrary degree.

3.1 Basis functions

In this subsection, we introduce a set of globally defined basis functions.

3.1.1 Classical polynomials and spherical harmonics

First, we give the definitions and the main properties of the associated Laguerre polynomials, associated Legendre polynomials, and of the spherical harmonics.

Associated Laguerre polynomials

The classical associated Laguerre polynomial of degree k is the polynomial solution of the differential equation

$$x\,y'' + (\alpha - 1 + x)\,y' + k\,y = 0\,, \quad \alpha \in \mathbb{R}_+\,.$$

It is denoted by $L_k^{(\alpha)}$. By the use of the abbreviation

$$\left(\begin{array}{c} k + \alpha \\ m \end{array}\right) = \frac{(k+\alpha)(k-1+\alpha)\ldots(k-m+\alpha)}{m!}\,,$$

an explicit formula for the polynomial $L_k^{(\alpha)}$ reads

$$L_k^{(\alpha)}(x) = \sum_{i=0}^{k}(-1)^i \left(\begin{array}{c} k + \alpha \\ k - i \end{array}\right) \frac{x^i}{i!}\,.$$

The orthogonality property of the associated Laguerre polynomials can be written as

$$\int_0^\infty x^\alpha \mathrm{e}^{-x} L_k^{(\alpha)}(x) L_m^{(\alpha)}(x)\,dx = \frac{\Gamma(k+1+\alpha)}{k!}\,\delta_{k,m}\,,$$

where $\delta_{k,m}$ is the Kronecker symbol. Thus, the polynomials are orthogonal with respect to the measure $x^\alpha \mathrm{e}^{-x}\,dx$. For numerical computations of the associated Laguerre polynomials, we use the initial functions

$$L_0^{(\alpha)}(x) = 1\,, \quad L_1^{(\alpha)}(x) = 1 + \alpha - x$$

and the following recursion for $k \geq 2$

$$L_k^{(\alpha)}(x) = \frac{(2k - 1 + \alpha - x)L_{k-1}^{(\alpha)}(x) - (k - 1 + \alpha)L_{k-2}^{(\alpha)}(x)}{k}\,.$$

Associated Legendre polynomials

The classical associated Legendre polynomial is the polynomial solution of the differential equation

$$(1 - x^2)\,y'' - 2x\,y' + \left(\ell(\ell+1) - \frac{m^2}{1 - x^2}\right) y = 0\,,$$

where the index ℓ is the degree and m the order of the associated Legendre polynomial $P_{\ell,m}$. An explicit formula for the polynomial $P_{\ell,m}$ is

$$P_{\ell,m}(x) = \frac{(-1)^m}{2^\ell\,\ell!}\,(1 - x^2)^{m/2}\frac{d^{\ell+m}}{dx^{\ell+m}}(x^2 - 1)^\ell\,, \quad 0 \leq m \leq \ell\,.$$

The orthogonality properties of the associated Legendre polynomials read as

$$\int_{-1}^{1} P_{\ell_1,m}(x) P_{\ell_2,m}(x)\,dx = 2\frac{(\ell+m)!}{(2\ell+1)(\ell-m)!}\,\delta_{\ell_1,\ell_2}\,,$$

for fixed m and, in the case $\ell_1 = \ell_2 = \ell$. Furthermore,

$$\int_{-1}^{1} \frac{1}{1-x^2} P_{\ell,m}(x) P_{\ell,k}(x)\,dx = \begin{cases} 0 & \text{for} \quad m \neq k \\ \dfrac{(\ell+m)!}{m(\ell-m)!} & \text{for} \quad k = m \neq 0 \end{cases}$$

for a fixed ℓ. For $k = m = 0$, the last integral diverges. For numerical evaluations of the associated Legendre polynomials, we use the initial functions

$$P_{m,m}(x) = (-1)^m (2m-1)!!\,(1-x^2)^{m/2}\,, \quad P_{m+1,m}(x) = x\,(2m+1)P_{m,m}(x)$$

and the following recursion for $k = m+2, \ldots, \ell$

$$P_{k,m}(x) = \frac{(2k-1)x P_{k-1,m}(x) - (k-1+m)P_{k-2,m}(x)}{k-m}\,.$$

Spherical harmonics

The spherical harmonics $Y_{\ell,m}$ are the complete and orthonormal set of eigenfunctions of the angular part of the three-dimensional Laplace's equation

$$\left(\frac{\partial^2}{\partial\theta^2} + \frac{\cos\theta}{\sin\theta}\frac{\partial}{\partial\theta} + \frac{1}{\sin^2\theta}\frac{\partial^2}{\partial\phi^2} \right) Y_{\ell,m}(\phi,\theta) = -\ell(\ell+1)Y_{\ell,m}(\phi,\theta)\,,$$

for $\ell \in \mathbb{N}_0$ and $m = -\ell, \ldots, 0, \ldots, \ell$. An explicit formula for the spherical harmonics with the parameterisation

$$e = \begin{pmatrix} \cos\phi\,\sin\theta \\ \sin\phi\,\sin\theta \\ \cos\theta \end{pmatrix} \tag{23}$$

is

$$Y_{\ell,m}(\phi,\theta) = \sqrt{\frac{2\ell+1}{4\pi}\frac{(\ell-m)!}{(\ell+m)!}}\; P_{\ell,m}(\cos\theta)\,e^{\imath\,m\phi}\,.$$

Here, $P_{\ell,m}$ are the associated Legendre polynomials. The orthogonality property of the spherical harmonics reads as

$$\int_{S^2} Y_{\ell_1,m_1}(e) Y_{\ell_2,m_2}(e)\,de = \delta_{\ell_1,\ell_2}\delta_{m_1,m_2}\,.$$

However, for our purposes, we will use the real valued version of the spherical harmonics in the form

$$Y_{\ell,m}(\phi,\theta) = \sqrt{\frac{2\ell+1}{2\pi}\frac{(\ell-m)!}{(\ell+m)!}}\; P_{\ell,m}(\cos\theta)\,\cos(m\phi)$$

for $m > 0$,

$$Y_{\ell,0}(\phi,\theta) = \sqrt{\frac{2\ell+1}{4\pi}}\; P_{\ell,0}(\cos\theta)$$

for $m = 0$ and

$$Y_{\ell,m}(\phi,\theta) = \sqrt{\frac{2\ell+1}{2\pi}\frac{(\ell-m)!}{(\ell+m)!}}\; P_{\ell,m}(\cos\theta)\,\sin(-m\phi)$$

for $m < 0$.

3.1.2 Basis functions

In three dimensional spherical coordinates

$$v = \varrho\, e_v\,, \quad 0 \le \rho < \infty\,, \ e_v \in S^2\,,$$

we decompose the basis function φ_j as follows

$$\varphi_j(v) = \varphi_j(\varrho\, e_v) = \Phi_{k,\ell}(\varrho)\, Y_{\ell,m}(e_v)\,, \quad k \in \mathbb{N}_0\,, \ \ell \in \mathbb{N}_0\,, \ -\ell \le m \le \ell\,.$$

Thus, the global index j is a function of three indices $j = (k, \ell, m)$. Since the angular part of the function φ_j is already defined, we look at the radial part and write the function Φ_k in the form

$$\Phi_{k,\ell}(\varrho) = \mu_{k,\ell}\, e^{-\varrho^2/2}\, L_k^{(\ell+1/2)}(\varrho^2)\, \varrho^\ell\,.$$

The normalisation parameters $\mu_{k,\ell}$ are chosen so, that the functions $\Phi_{k,\ell}$ will compose an orthonormal system with respect to the measure $\varrho^2\, d\varrho$. Setting $\varrho^2 = x$, $2\varrho\, d\varrho = dx$, we get

$$\int_0^\infty \mu_{k_1,\ell}\mu_{k_2,\ell}\, \varrho^{2\ell+2}\, e^{-\varrho^2}\, L_{k_1}^{(\ell+1/2)}(\varrho^2) L_{k_2}^{(\ell+1/2)}(\varrho^2)\, d\varrho =$$

$$\frac{1}{2}\, \mu_{k_1,\ell}\mu_{k_2,\ell} \int_0^\infty \varrho^{2\ell+1} e^{-\varrho^2}\, L_{k_1}^{(\ell+1/2)}(\varrho^2) L_{k_2}^{(\ell+1/2)}(\varrho^2)\, 2\varrho\, d\varrho =$$

$$\frac{1}{2}\mu_{k_1,\ell}\mu_{k_2,\ell} \int_0^\infty x^{\ell+1/2} e^{-x}\, L_{k_1}^{(\ell+1/2)}(x) L_{k_2}^{(\ell+1/2)}(x)\, dx =$$

$$\frac{1}{2}\, \mu_{k,\ell}^2\, \frac{\Gamma(k+\ell+3/2)}{k!}\, \delta_{k_1,k_2}\,,$$

in the case $k_1 = k_2 = k$. To obtain an orthonormal system, we set

$$\mu_{k,\ell} = \sqrt{\frac{2\, k!}{\Gamma(k+\ell+3/2)}}\,.$$

This yields the form of the function $f^{(n)}$ in spherical coordinates $v = \varrho\, e_v$

$$f^{(n)}(v) = \sum_{k=0}^K \sum_{\ell=0}^L \sum_{m=-\ell}^\ell f_{k,\ell,m} \Phi_{k,\ell}(\varrho)\, Y_{\ell,m}(e_v)\,.$$

The number of the basis functions is

$$n = (K+1)\,(L+1)^2\,.$$

3.2 Test functions

All basis functions belong to the Schwartz space $\mathbb{S}$ of infinitely smooth functions all of whose derivatives are rapidly decreasing. Thus the collision integral $Q(\varphi_k, \varphi_\ell)$ is a Schwartz function as well and, therefore, any tempered distribution can be chosen as a test function ψ_i. In the case of regular distribution ψ_i identified with a continuous function

$$\psi_i \; : \; \mathbb{R}^3 \to \mathbb{R} \,,$$

the entries of the matrices Q_i can be evaluated for $i, k, \ell = 1, \ldots, n$ as follows

$$Q_i[k, \ell] = <Q(\varphi_k, \varphi_\ell), \psi_i> = \int\limits_{\mathbb{R}^3} Q(\varphi_k, \varphi_\ell)(v) \psi_i(v) \, dv$$

$$= \; \frac{1}{2} \int\limits_{\mathbb{R}^3} \int\limits_{\mathbb{R}^3} \varphi_k(v) \varphi_\ell(w) \int\limits_{S^2} B(v, w, e) \Big(\psi_i(v') + \psi_i(w') - \psi_i(v) - \psi_i(w) \Big) de \, dw \, dv,$$

where the weak form of the collision integral (8) has been used. If the set of test functions contains a collision invariant, the corresponding matrices Q_i will vanish completely, and, the corresponding macroscopic quantity will be conserved automatically.

One possible choice is a pure Galerkin method with

$$\psi_i = \varphi_i \,, \quad i = 1, \ldots, n \,.$$

In this case, the mass matrix M is the identity matrix due to the orthogonality of the system. However, an additional numerical conservation procedure is necessary. Due to an automatic fulfilment of the conservation properties, the following choice of test functions for a index $i = (k, \ell, m)$ seems to be natural

$$\psi_i(v) = L_k^{(\ell + 1/2)}(\varrho^2) \, \varrho^\ell \, Y_{\ell, m}(e_v) \,, \quad \text{for } v = \varrho \, e_v \,.$$

These globally defined polynomials are in fact the basis functions without the factor $\mu_{k, \ell} \, \mathrm{e}^{-\varrho^2/2}$. All five collision invariants are included in the set of the test functions, namely

$$\psi_{0,0,0}(v) \;=\; \sqrt{\frac{1}{4\,\pi}} \,,$$

$$\psi_{0,1,-1}(v) \;=\; \sqrt{\frac{3}{4\,\pi}} \, \varrho \, \sin\phi \, \sin\theta = \sqrt{\frac{3}{4\,\pi}} \, v_2 \,,$$

$$\psi_{0,1,0}(v) \;=\; \sqrt{\frac{3}{4\,\pi}} \, \varrho \, \cos\theta = \sqrt{\frac{3}{4\,\pi}} \, v_3 \,,$$

$$\psi_{0,1,1}(v) \;=\; \sqrt{\frac{3}{4\,\pi}} \, \varrho \, \cos\phi \, \sin\theta = \sqrt{\frac{3}{4\,\pi}} \, v_1 \,,$$

$$\psi_{1,0,0}(v) \;=\; \sqrt{\frac{1}{4\,\pi}} \Big(-\varrho^2 + \frac{3}{2} \Big) = \sqrt{\frac{1}{4\,\pi}} \Big(-|v|^2 + \frac{3}{2} \Big) \,.$$

Thus, the conservation properties are now ensured automatically.

For a regular Galerkin-Petrov scheme, it is necessary to choose the same number of basis and test functions, i.e. for

$$k = 0, \ldots, K, \ \ell = 0, \ldots, L, \ -\ell \le m \le \ell,$$

we get

$$n = (K+1)(L+1)^2.$$

3.3 Mass matrix

The mass matrix $M \in \mathbb{R}^{n \times n}$ has the entries

$$M[i,j] = < \varphi_j, \psi_i >, \quad i, j = 1, \ldots, n,$$

where $i = (k_i, \ell_i, m_i)$ and $j = (k_j, \ell_j, m_j)$. Since both, basis and test functions contain spherical harmonics which are mutually orthonormal, in spherical coordinates we obtain

$$M[i,j] = 0, \quad \text{for } \ell_i \ne \ell_j \text{ or } m_i \ne m_j$$

and

$$M[i,j] = \mu_{k_j,\ell} \int\limits_0^\infty \varrho^{2\ell+2} \mathrm{e}^{-\varrho^2/2} L_{k_j}^{(\ell+1/2)}(\varrho^2) L_{k_i}^{(\ell+1/2)}(\varrho^2) \, d\varrho \tag{24}$$

for $\ell_i = \ell_j = \ell$ and $m_i = m_j = m$. Thus, the mass matrix is rather sparse and, since $M[i,j]$ do not depend on m, has many equal non-zero entries.

3.4 Collision matrices

For a general interaction model, the collision matrices Q_i have the entries

$$Q_i[k,\ell] = \int\limits_{\mathbb{R}^3} \int\limits_{\mathbb{R}^3} \varphi_k(v)\varphi_\ell(w) q_i(v,w) \, dw \, dv, \tag{25}$$

where

$$q_i(v,w) = \int\limits_{S^2} B(v,w,e) \Big(\psi_i(v') + \psi_i(w') - \psi_i(v) - \psi_i(w) \Big) de. \tag{26}$$

The integration (26) is an important part of the generation of the collision matrices. For the VHS model of interaction (10), and for general polynomial test functions, this integration can be done analytically leading to a function q_i which is a polynomial in six variables v and w multiplied by $|u|^\lambda$. For more general models of interaction and for test functions given in spherical coordinates an analytic integration seems to be impossible. Furthermore, for the non cut-off collision models, the kernel B has a singularity and the corresponding numerical integration should be done very carefully.

4 Numerical realisation

The main advantage of the above Galerkin-Petrov method is the possibility to pre-compute and to store all the collision matrices Q_i and the mass matrix M for different discretisation parameters K and L. Furthermore, these matrices are also independent of a time discretisation scheme and corresponding time discretisation parameters. Therefore, once computed, experiments with different time discretisation schemes can be easily performed. For the numerical integration over $\mathbb{R}^3$, we will use spherical coordinates and a combination of the radial Gauss-Laguerre quadratures with the Lebedev quadratures for the integration over the unit sphere. For a given function $g : \mathbb{R}_+ \to \mathbb{R}$, the Gauss-Laguerre quadrature is applied to the integrals of the form

$$I[g] = \int_0^\infty x^{1/2} \mathrm{e}^{-x}\, g(x)\, dx$$

and results in an approximation

$$I_{N_{GL}}[g] = \sum_{i=1}^{N_{GL}} \omega_i^{GL}\, g(x_i)\,.$$

The weights ω_i^{GL} and the positions x_i are available for any N_{GL} with an arbitrary accuracy (see [44]). By the use of the parameterisation (23), the integral over the unit sphere for a given function $g : S^2 \to \mathbb{R}$

$$I[g] = \int_{S^2} g(e)\, de$$

can be transformed into the corresponding integrals over the rectangular domain $[0, 2\pi] \times [0, \pi]$ and subject to the subsequent application of the classical Gauss quadratures. However, the Lebedev quadratures [31],[32]

$$I[g] = 4\pi \sum_{j=1}^{N_L} \omega_j^L\, g(e_j)\,, \quad e_j \in S^2$$

are invariant under finite rotation groups and available for many values of N_L. The first of them are for $N_L = 6, 14, 26, 38, 50, 74, 86, 110$. We claim that this set will be sufficient for our first tests.

Mass matrix

The Gauss-Laguerre quadratures will be used for numerical computation of the mass matrix entries corresponding to (24). With the substitution $\varrho^2 = x$, $2\varrho\, d\varrho = dx$, we get

$$M[i, j] = \frac{1}{2}\, \mu_{k_j,\ell} \int_0^\infty x^{\ell+1/2} \mathrm{e}^{-x} \left(x^\ell \mathrm{e}^{x/2}\, L_{k_j}^{(\ell+1/2)}(x)\, L_{k_i}^{(\ell+1/2)}(x) \right) dx$$

14

and approximate these entries as

$$M_{N_{GL}}[i,j] = \frac{1}{2}\,\mu_{k_j,\ell} \sum_{i_v=1}^{N_{GL}} \omega_{i_v}^{GL}\,x_{i_v}^{\ell}\,\mathrm{e}^{x_{i_v}/2}\,L_{k_j}^{(\ell+1/2)}(x_{i_v})\,L_{k_i}^{(\ell+1/2)}(x_{i_v})\,.$$

As we have mentioned before, only few entries of the mass matrix are different from zero and they are computed numerically during the initialisation. This requires just a few seconds of computer time. Then we use LAPACK package to perform the LU decomposition of the matrix $M_{N_{GL}}$ in order to solve the systems of linear equations with the mass matrix in initial and later in every time step of the algorithm. Formally, the numerical work for this decomposition is $\mathcal{O}(n^3)$. However, the corresponding computer time is negligible in our experiments.

Collision matrices

The computation of the collision matrices is the most important and numerically difficult step of the algorithm. However, it is an initialisation step and will be done only once for the given collision kernel and for the fixed parameters K, L, N_{GL} and N_L. Then all n collision matrices of the dimension $n \times n$ will be stored and used for all computations on the later stages. By the use of the substitution $\varrho^2 = x$, $2\,\varrho\,d\varrho = dx$ again, we get for a function $g : \mathbb{R}^3 \to \mathbb{R}$

$$
\begin{aligned}
I[g] = \int_{\mathbb{R}^3} g(v)\,dv &= \int_0^\infty \varrho^2 \int_{S^2} g(\varrho\,e)\,de\,d\varrho \\
&= \frac{1}{2}\int_0^\infty x^{1/2}\mathrm{e}^{-x}\left(\mathrm{e}^x \int_{S^2} g(\sqrt{x}\,e)\,de\right) dx
\end{aligned}
$$

and approximate these integrals as follows

$$I_{N_{GL},N_L}[g] = 2\,\pi \sum_{i_v=1}^{N_{GL}} \omega_{i_v}^{GL}\mathrm{e}^{x_{i_v}} \sum_{j_v=1}^{N_L} \omega_{j_v}^{L} g(\sqrt{x_{i_v}}\,e_{j_v})\,.$$

Thus, for the entries of the collision matrices $Q_l[k,\ell]$ with $k = (k_v, \ell_v, m_v)$ and $\ell = (k_w, \ell_w, m_w)$ we get

$$
\begin{aligned}
\left(Q_{N_{GL},N_L}\right)_i[k,\ell] = (2\,\pi)^2 \sum_{i_v=1}^{N_{GL}} &\omega_{i_v}^{GL}x_{i_v}^{\ell_v}\mathrm{e}^{x_{i_v}/2}\,L_{k_v}^{(\ell_v+1/2)}(x_{i_v}) \times \\
&\sum_{j_v=1}^{N_L} \omega_{j_v}^{L} Y_{\ell_v,m_v}(e_{j_v}) \times \\
&\sum_{i_w=1}^{N_{GL}} \omega_{i_w}^{GL}x_{i_w}^{\ell_v}\mathrm{e}^{x_{i_w}/2}\,L_{k_w}^{(\ell_w+1/2)}(x_{i_w}) \times \\
&\sum_{j_w=1}^{N_L} \omega_{j_w}^{L} Y_{\ell_w,m_w}(e_{j_w})\left(q_L\right)_i(v_{i_v,j_v}, w_{i_w,j_w})\,,
\end{aligned}
$$

15

where $v_{i_v,j_v} = \sqrt{x_{i_v}}e_{j_v}$, $w_{i_w,j_w} = \sqrt{x_{i_w}}e_{j_w}$ and

$$\left(q_L\right)_i(v_{i_v,j_v}, w_{i_w,j_w}) = \sum_{j=1}^{N_L} \omega_j^L B(v_{i_v,j_v}, w_{i_w,j_w}, e_j) \times$$

$$\left(\psi_i(v'_{i_v,j_v,i_w,j_w}(e_j)) + \psi_i(w'_{i_v,j_v,i_w,j_w}(e_j)) - \psi_i(v_{i_v,j_v}) + \psi_i(w_{i_w,j_w})\right),$$

with

$$v'_{i_v,j_v,i_w,j_w}(e_j) = \frac{v_{i_v,j_v} + w_{i_w,j_w}}{2} + \frac{1}{2}|v_{i_v,j_v} - w_{i_w,j_w}|e_j,$$

$$w'_{i_v,j_v,i_w,j_w}(e_j) = \frac{v_{i_v,j_v} + w_{i_w,j_w}}{2} - \frac{1}{2}|v_{i_v,j_v} - w_{i_w,j_w}|e_j.$$

It is clear that it impossible to compute all these matrices by the direct use of the above formulae for reasonable discretisation parameters. However, the separated structure of the factors allows to precompute three arrays P_{GL}, P_L and P_Q and to use them to assemble the collision matrices in an efficient manner. The components of the first array are for $k = 0, \ldots, K$, $\ell = 0, \ldots, L$ and $i = 1, \ldots, N_{GL}$

$$\left(P_{GL}\right)_{k,\ell,i} = \omega_i^{GL} x_i^\ell e^{x_i/2} L_k^{(\ell+1/2)}(x_i)$$

leading to $(K+1)(L+1)N_{GL}$ words of computer memory. The components of the second array are for $\ell = 0, \ldots, L$, $m = -\ell, \ldots, \ell$ and $j = 1, \ldots, N_L$

$$\left(P_L\right)_{l,m,j} = \omega_j^L Y_{\ell,m}(e_j)$$

leading to $(L+1)^2 N_L$ words of computer memory. Finally, the most complicated array is

$$\left(P_Q\right)_{i_v,j_v,i_w,j_w,i} = \left(q_L\right)_i(v_{i_v,j_v}, w_{i_w,j_w})$$

leading to $n N_{GL}^2 N_L^2$ words of computer memory. The numerical cost of the first two arrays is sub-linear in n and requires a negligible computer time. The computation of the third array, however, is more demanding. Formally, it requires only a linear amount of operations with respect to the number of unknowns and quadratic with respect to the number of integration points. However, these numbers are not independent and in order to keep the spectral accuracy, an increase of the number of integration points is unavoidable with increasing n. The computations of all Q_i, $i = 1, \ldots, n$ is as follows

$$\left(Q_{N_{GL},N_L}\right)_i[k,\ell] = (2\pi)^2 \sum_{i_v=1}^{N_{GL}} \sum_{j_v=1}^{N_L} \sum_{i_w=1}^{N_{GL}} \sum_{j_w=1}^{N_L} \alpha_{i_v,j_v,i_w,j_w} \left(P_Q\right)_{i_v,j_v,i_w,j_w,i}$$

where

$$\alpha_{i_v,j_v,i_w,j_w} = \left(P_{GL}\right)_{k_v,l_v,i_v} \left(P_L\right)_{l_v,m_v,j_v} \left(P_{GL}\right)_{k_w,l_w,i_w} \left(P_L\right)_{l_w,m_w,j_w}.$$

16

Note that $\alpha_{i_v, j_v, i_w, j_w}$ is independent of i and, therefore, once computed, can be used to update the i_v, j_v, i_w, j_w sum for all matrices i. This leads to only a few multiplications and additions for the entries of the collision matrices without evaluation of special functions. The numerical work and memory, however, is still of the order $\mathcal{O}(n^3)$. Furthermore, the entries k, ℓ of the collision matrices are independent from each other and, therefore, their computation can be done in parallel by the use of the open MP software without any additional programming effort.

Time discretisation

Once the mass matrix M and all collision matrices Q_i are computed (from now on the subscripts N_{GL} and N_L are omitted), we can start a numerical solution of the problem. First of all, the initial right hand side $\underline{f}_0$ has to be computed

$$\left(\underline{f}_0\right)_i = < f_0, \psi_i >, \quad i = 1, \ldots, n.$$

We use the numerical quadrature

$$\left(\underline{f}_0\right)_i = 2\,\pi \sum_{i_v=1}^{N_{GL}} \omega_{i_v}^{GL} \mathrm{e}^{x_{i_v}} \sum_{j_v=1}^{N_L} \omega_{j_v}^L f_0\big(\sqrt{x_{i_v}}\,e_{j_v}\big)\,\psi_i\big(\sqrt{x_{i_v}}\,e_{j_v}\big), \quad i = 1, \ldots, n$$

and compute the initial coefficient vector

$$\underline{f}^{(0)} = M^{-1} \underline{f}_0.$$

Then we choose a time step $\tau > 0$ and the final time $T = \tau\,N_t$. For the time integration of the system (22), we can choose any classical solver, for example the most simple Euler scheme or the Runge-Kutta method of the second or a higher order. For the Euler method the kth step, $k = 0, \ldots, N_t - 1$, is as follows. Compute the vector $\underline{q}$ with

$$\underline{q}_i = (Q_i \underline{f}^{(k)}, \underline{f}^{(k)}), \quad i = 1, \ldots, n$$

by the use of the BLAS library. Compute the next coefficient vector $\underline{f}^{(k+1)}$ as

$$\underline{f}^{(k+1)} = \underline{f}^{(k)} + \tau\,M^{-1} \underline{q}$$

by utilising the functionality of the LAPACK package and the BLAS library once again.

5 Numerical examples

In this section we consider three examples of relaxation. The collision kernel of the first two examples will be constant, i.e.

$$B(v, w, e) = \frac{1}{4\,\pi}.$$

This is the most simple case of Maxwell pseudo–molecules. For this kernel, the exact relaxation time of any moment of the distribution function is known. Thus, we will

be able to check the accuracy of our scheme very carefully. In the first example, we will consider a sum of two Maxwell distributions as an initial condition. The second example is the famous BKW solution for which not only the time relaxation of the moments but the distribution function itself is analytically known. However, this solution is an isotropic function and, therefore, its numerical approximation by our spectral scheme is rather simple. The third example will be the classical hard spheres model with the collision kernel

$$B(v, w, e) = \frac{1}{4\pi} |v - w|.$$

No analytic dependencies are available for this example. Thus, we will compare our results with those obtained by the use of a stochastic particle method.

5.1 Relaxation of a mixture of two Maxwellian's

For the spatially homogeneous relaxation, the density, the mean velocity and the temperature

$$\rho = \int_{\mathbb{R}^3} f(t, v)\, dv\,, \quad V = \frac{1}{\rho} \int_{\mathbb{R}^3} v\, f(t, v)\, dv\,, \quad T = \frac{1}{3\rho} \int_{\mathbb{R}^3} |v - V|^2\, f(t, v)\, dv$$

are conserved quantities. The relaxation of the flow of momentum, the flow of energy and of the special fourth moment

$$M(t) = \int_{\mathbb{R}^3} vv^\top f(t, v)\, dv\,, \quad r(t) = \int_{\mathbb{R}^3} v|v|^2\, f(t, v)\, dv\,, \quad s(t) = \int_{\mathbb{R}^3} |v|^4\, f(t, v)\, dv$$

is given as in [42] by

$$
\begin{aligned}
M(t) &= M_0\, e^{-t/2} + \left(T\, I + VV^\top\right)\left(1 - e^{-t/2}\right), &&(27)\\
r(t) &= r_0\, e^{-t/3} + \left(5\, T + |V|^2\right) V \left(1 - e^{-t/3}\right)\\
&\quad + 2\left(M_0 - VV^\top - T\, I\right) V \left(e^{-t/2} - e^{-t/3}\right),\\
s(t) &= s_0\, e^{-t/3} + \left(|V|^4 + 15\, T^2 + 10\, T\, |V|^2\right)\left(1 - e^{-t/3}\right) &&(28)\\
&\quad + \frac{1}{2}\left(\|M_0\|_F^2 - 3\, T^2 + |V|^4 - 2(M_0 V, V)\right)\left(e^{-t} - e^{-t/3}\right)\\
&\quad + 4\left((M_0 V, V) - |V|^4 - T\, |V|^2\right)\left(e^{-t/2} - e^{-t/3}\right),
\end{aligned}
$$

where

$$M_0 = \int_{\mathbb{R}^3} vv^\top f_0(v)\, dv\,, \quad r_0 = \int_{\mathbb{R}^3} v|v|^2\, f_0(v)\, dv\,, \quad s_0 = \int_{\mathbb{R}^3} |v|^4\, f_0(v)\, dv$$

and $\|\cdot\|_F$ denotes the Frobenius norm. We will consider the initial distribution f_0 in the form of a convex sum of two Maxwell distributions

$$f_0(v) = \alpha f_{M_1}(v) + (1 - \alpha)f_{M_2}(v)\,, \quad 0 \le \alpha \le 1\,, \tag{29}$$

18

where

$$f_{M_i}(v) = \frac{1}{(2\pi\, T_i)^{3/2}}\, \mathrm{e}^{-\dfrac{|v - V_i|^2}{2\, T_i}}\,, \quad i = 1, 2\,.$$

In these settings, the initial values are

$$\begin{aligned}
\rho &= 1\,,\\
V &= \alpha V_1 + (1-\alpha)V_2\,,\\
T &= \alpha T_1 + (1-\alpha)T_2 + \frac{1}{3}\alpha(1-\alpha)|V_1 - V_2|^2\,,\\
M_0 &= \alpha\left(T_1\, I + V_1 V_1^{\top}\right) + (1-\alpha)\left(T_2\, I + V_2 V_2^{\top}\right)\,,\\
r_0 &= \alpha\left(5T_1 + |V_1|^2\right)V_1 + (1-\alpha)\left(5T_2 + |V_2|^2\right)V_2\,,\\
s_0 &= \alpha\left(|V_1|^4 + 15\, T_1^2 + 10\, T_1\, |V_1|^2\right) +\\
&\quad (1-\alpha)\left(|V_2|^4 + 15\, T_2^2 + 10\, T_2\, |V_2|^2\right)\,.
\end{aligned}$$

For our first example, we choose

$$\alpha = 1/2\,,\; V_1 = (-1, 0, 0)^{\top}\,, \quad V_2 = (+1, 0, 0)^{\top}\,, \quad T_1 = T_2 = \frac{2}{3}$$

and obtain

$$V = (0, 0, 0)^{\top}\,, \quad T = 1\,.$$
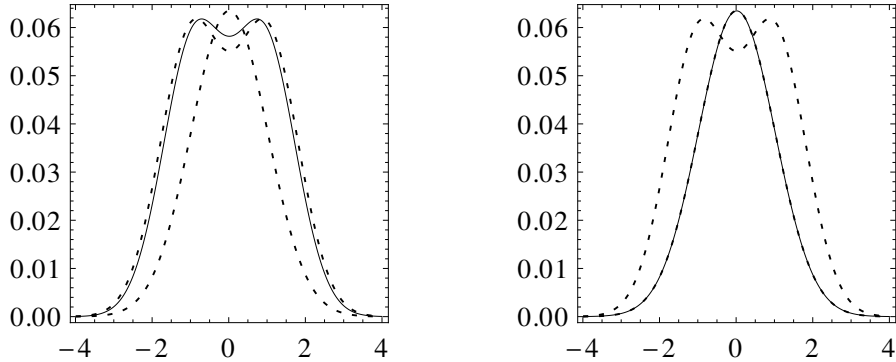
Figure 1: Initial and final distributions for $n = 27$

Initial condition

For a series of discretisation parameters K and L, we first define the parameters of the Gauss-Laguerre and Lebedev quadratures N_{GL} and N_L in the following way. We perform approximation of the initial condition and choose the minimal values of N_{GL} and N_L leading to the highest approximation quality for the given values of K and L. In the first two figures we illustrate the approximation of the initial condition $f_0(v_1, 0, 0)$, $v_1 \in [-4, 4]$ and of the final Maxwell distribution $f_M(v_1, 0, 0)$, $v_1 \in [-4, 4]$ for $K = L = 2$ with $n = 27$ basis functions (Figure 1) and for $K = L = 4$ with $n = 125$ basis functions (Figure 2). The initial condition and the final Maxwell distribution are shown with thick dashed lines, while the numerical approximation is depicted by the thin solid line. There is a clear numerical error by the approximation of the initial condition for $n = 27$. For $n = 125$, however, the error can not be optically seen on the figure. The final Maxwell distribution is perfectly approximated in both cases. The $L_2(\mathbb{R}^3)$ error

$$\frac{\|f^{(n)}(0, \cdot) - f_0\|_{L_2(\mathbb{R}^3)}}{\|f_0\|_{L_2(\mathbb{R}^3)}}$$

of the approximation of the initial condition f_0 is summarised in Table 1 and its logarithmic plot is shown in Figure 3. The last column in Table 1 contains the Convergence Factor (CF), i.e. a quotient of two consecutive errors. The exponential convergence of the error is clearly seen.
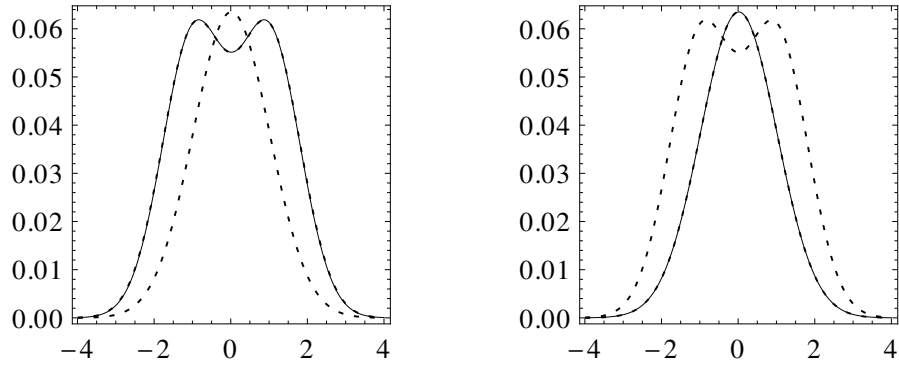
Figure 2: Initial and final distributions for $n = 125$

Table 1: Approximation error for the initial condition

K	L	n	N_L	N_{GL}	$L_2(\mathbb{R}^3)$-Norm	CF
2	2	27	38	8	$5.07 \cdot 10^{-2}$	-
4	4	125	50	8	$3.45 \cdot 10^{-3}$	14.7
6	6	343	110	16	$2.51 \cdot 10^{-4}$	13.7
8	8	729	110	16	$1.72 \cdot 10^{-5}$	14.6
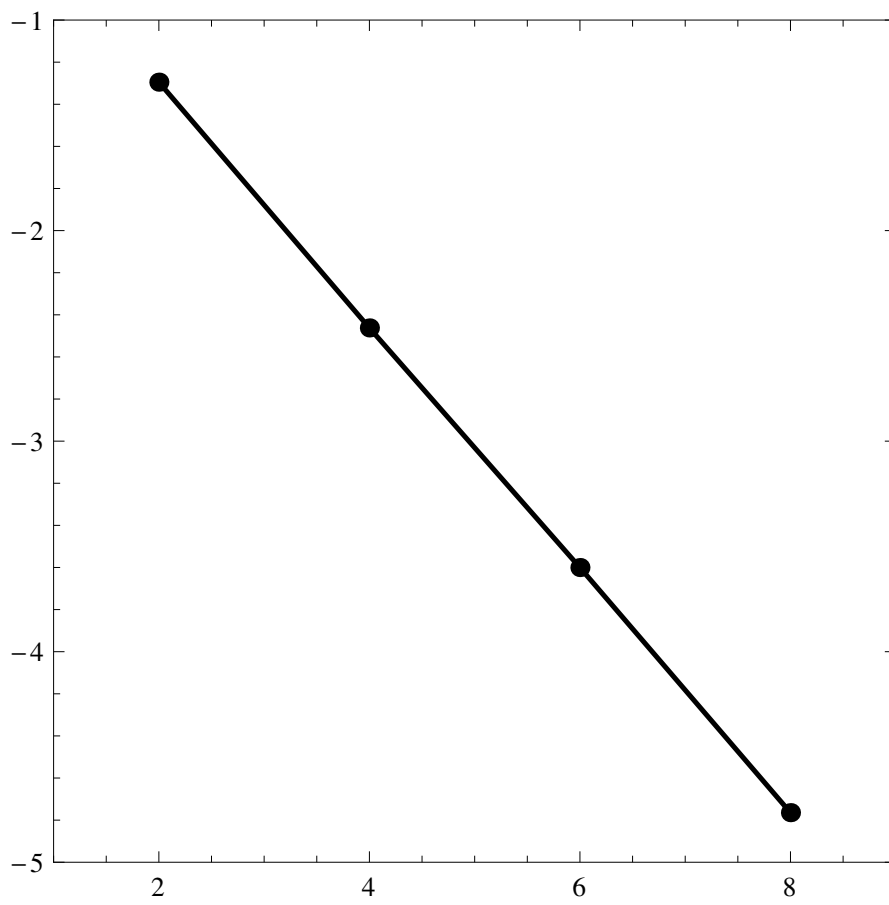
Figure 3: $\log_{10}$ course of the $L_2(\mathbb{R}^3)$ error
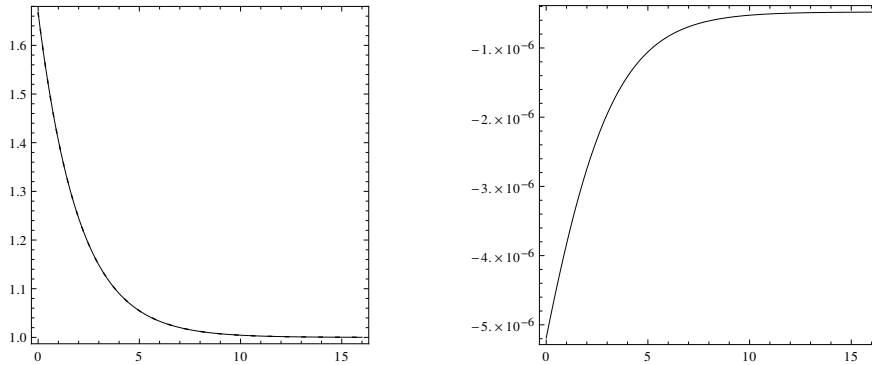
Figure 4: Course of the functional $M_{11}(t)$
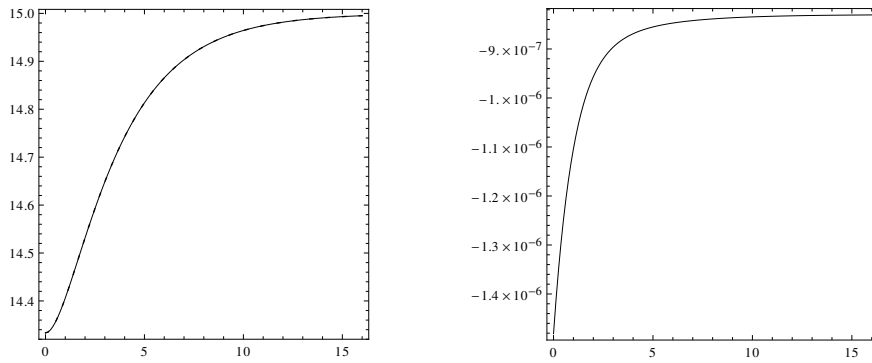
Figure 5: Course of the functional $s(t)$

Relaxation of the moments

In the study of the accuracy of the time dependent moments of the distribution function, two new aspects have to be considered, namely the value of the time discretisation parameter τ and the quality of the time integrating scheme. We will demonstrate the efficiency of the simplest Euler scheme and of the Runge-Kutta method of orders two and four. For the given example, there is a non-trivial relaxation of the main diagonal components of the flux of momentum tensor (27) and of the fourth moment (28). Figure 4 shows the course of the function $M_{11}(t)$ where the thick dashed line is the analytic solution and the thin solid line is the computed moment for $n = 125$. There is no optical difference. The time relaxation of the function $s(t)$ is shown in Figure 5. The right plots on both figures show the time evolution of the difference between the analytic and the numerical solutions.

In the next three tables we present the maximal error for these moments computed with different time steps on the time interval $[0, 16]$ for different values of n. The

23

Table 2: Error for the moments $M_{11}(t)$ and $s(t)$, Euler method

N_t	n	$M_{11}(t)$	CF	$s(t)$	CF
32	27	$2.78 \cdot 10^{-2}$	-	$1.75 \cdot 10^{-3}$	-
64	27	$1.33 \cdot 10^{-2}$	2.09	$8.01 \cdot 10^{-4}$	2.18
128	27	$6.61 \cdot 10^{-3}$	2.01	$4.13 \cdot 10^{-4}$	1.94
256	**27**	$\mathbf{3.37 \cdot 10^{-3}}$	**1.96**	$\mathbf{2.40 \cdot 10^{-4}}$	**1.72**
256	125	$3.17 \cdot 10^{-3}$	-	$1.61 \cdot 10^{-4}$	-
512	125	$1.58 \cdot 10^{-3}$	2.01	$7.98 \cdot 10^{-5}$	2.02
1024	125	$7.89 \cdot 10^{-4}$	2.00	$4.01 \cdot 10^{-5}$	1.99
2048	125	$3.95 \cdot 10^{-4}$	2.00	$2.05 \cdot 10^{-5}$	1.96
4096	125	$1.99 \cdot 10^{-4}$	1.98	$1.08 \cdot 10^{-5}$	1.90
8192	**125**	$\mathbf{1.00 \cdot 10^{-4}}$	**1.99**	$\mathbf{5.98 \cdot 10^{-6}}$	**1.81**

Table 3: Error for the moments $M_{11}(t)$ and $s(t)$, Runge-Kutta 2

N_t	n	$M_{11}(t)$	CF	$s(t)$	CF
32	27	$2.34 \cdot 10^{-3}$	-	$2.63 \cdot 10^{-4}$	-
64	**27**	$\mathbf{4.16 \cdot 10^{-4}}$	**5.63**	$\mathbf{9.93 \cdot 10^{-5}}$	**4.19**
64	125	$5.72 \cdot 10^{-4}$	-	$7.49 \cdot 10^{-5}$	-
128	125	$1.34 \cdot 10^{-4}$	4.27	$1.68 \cdot 10^{-5}$	4.46
256	125	$3.11 \cdot 10^{-5}$	4.31	$3.26 \cdot 10^{-6}$	5.15
512	**125**	$\mathbf{6.03 \cdot 10^{-6}}$	**5.16**	$\mathbf{1.48 \cdot 10^{-6}}$	**2.20**
1024	343	$2.05 \cdot 10^{-6}$	-	$2.63 \cdot 10^{-7}$	-
2048	343	$5.12 \cdot 10^{-7}$	4.00	$6.55 \cdot 10^{-8}$	4.05
4096	343	$1.27 \cdot 10^{-7}$	4.03	$1.63 \cdot 10^{-8}$	4.02
8192	**343**	$\mathbf{3.19 \cdot 10^{-8}}$	**3.98**	$\mathbf{4.07 \cdot 10^{-9}}$	**4.00**

lines indicated in bold, shows the best accuracy reached for the given value of n and for a maximal number of time steps $N_t \leq 8192$. The linear, quadratic and fourth order convergences in time for different time integration schemes are evident. In the last table, we observe no proper convergence of the finest discretisation with $n = 729$. The errors for $N_t = 128, 256$ is practically identical to those obtained for $n = 343$. For $N_t = 512$, the error for M_{11} practically jumps to the machine accuracy, while the error for s increases. This is a clear indicator that the numerical integration with $N_{LG} = 16$ and $N_L = 110$ is not sufficiently accurate to yield the theoretically achievable high accuracy for this n.

H-functional and convergence to equilibrium

In Figures 6 and 7, we show the plots of the numerical density function $f^{(n)}(t, v_1, v_2, 0)$ and its contours for $(v_1, v_2) \in [-4, 4] \times [-4, 4]$ with 32×32 points and for the times $t = 0, 1/4, 1, 16$ obtained for $n = 125$.

Table 4: Error for the moments $M_{11}(t)$ and $s(t)$, Runge-Kutta 4

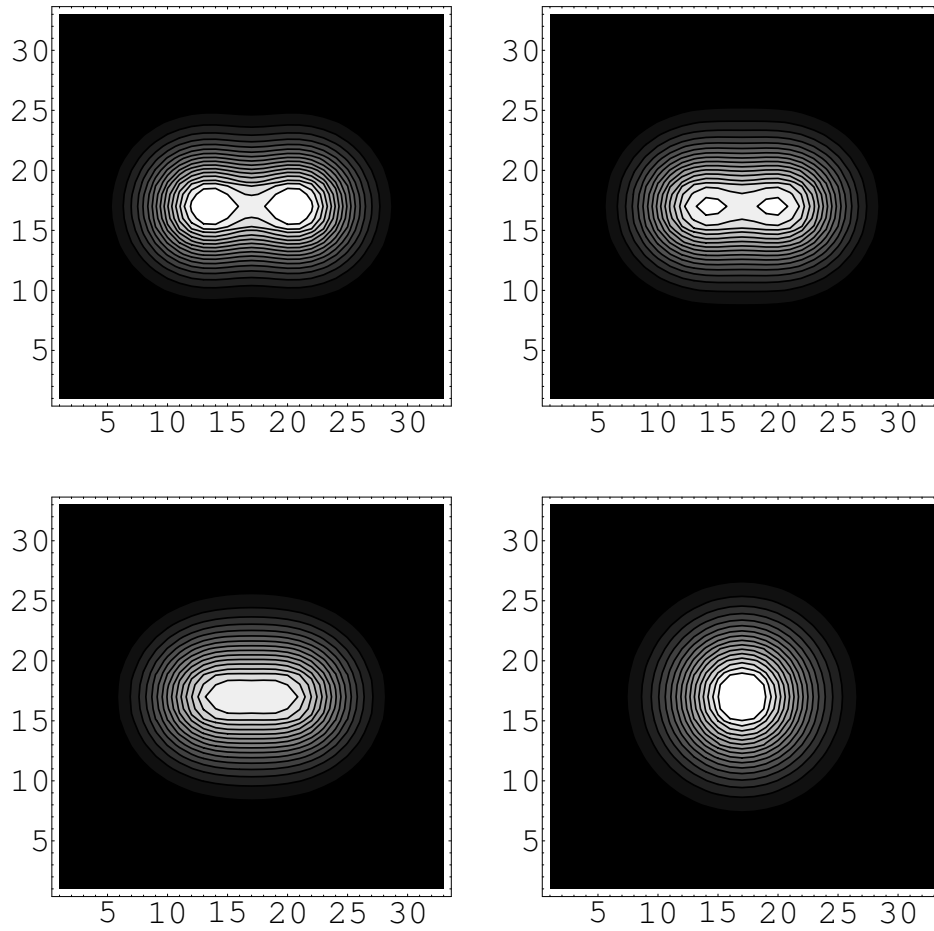| N_t	n	$M_{11}(t)$	CF	$s(t)$	CF
32	**27**	$\mathbf{4.16 \cdot 10^{-4}}$	**-**	$\mathbf{4.20 \cdot 10^{-4}}$	**-**
32	**125**	$\mathbf{5.81 \cdot 10^{-6}}$	**-**	$\mathbf{5.41 \cdot 10^{-6}}$	**-**
64	343	$4.53 \cdot 10^{-7}$	-	$2.18 \cdot 10^{-8}$	-
128	343	$2.68 \cdot 10^{-8}$	16.9	$1.28 \cdot 10^{-9}$	17.0
256	343	$1.58 \cdot 10^{-9}$	17.0	$6.33 \cdot 10^{-11}$	20.2
512	**343**	$\mathbf{1.36 \cdot 10^{-10}}$	**9.41**	$\mathbf{2.43 \cdot 10^{-11}}$	**2.61**
128	729	$2.68 \cdot 10^{-8}$	-	$1.28 \cdot 10^{-9}$	-
256	729	$1.58 \cdot 10^{-9}$	17.0	$6.32 \cdot 10^{-11}$	20.2
512	**729**	$\mathbf{1.71 \cdot 10^{-14}}$	**-**	$\mathbf{1.63 \cdot 10^{-9}}$	**-**
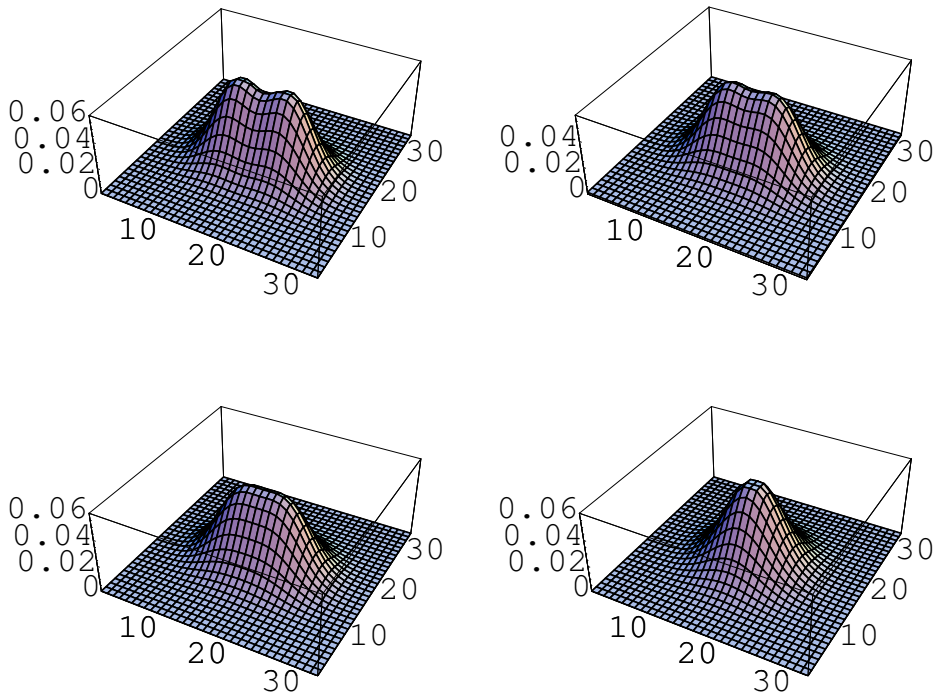
Figure 6: Density function for $t = 0, 1/4, 1, 16$

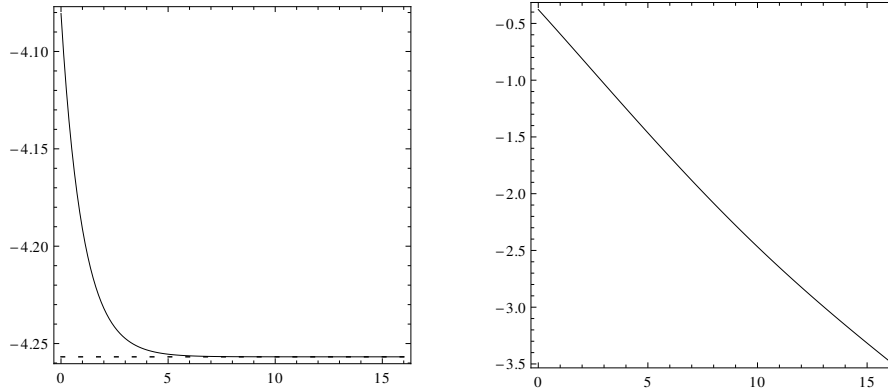Figure 7: Contours of the density function for $t = 0, 1/4, 1, 16$

Figure 8: Course of the H-functional and of the L_2−error for $n = 343$

Finally, in Figure 8, we show the time relaxation of the numerical Boltzmann H-functional (left plot)

$$H(t) = \int_{\mathbb{R}^3} f^{(n)}(t, v) \ln f^{(n)}(t, v) \, dv$$

for $n = 125$. Its analytically known asymptotic value

$$\lim_{t \to \infty} H(t) = \ln \frac{1}{(2\,\pi)^{3/2}} - \frac{3}{2} = -4.25681\ldots.$$

is shown as a dashed thick line, while the course of the H-functional is depicted by the thin solid line. The right plot in Figure 8 shows the $\log_{10}$-course of the relative L_2-norm of the difference of the current distribution function to the final Maxwell distribution.

$$\frac{\|f^{(n)}(t, \cdot) - f_M\|_{L_2(\mathbb{R}^3)}}{\|f_M\|_{L_2(\mathbb{R}^3)}}$$

which obviously shows exponential convergence.

5.2 BKW solution

In this subsection, we consider the famous exact solution of the Boltzmann equation found by Bobylev [9] and Krook and Wu [30]. The solution is obtained for $\lambda = 0$ in (7) and is of the form

$$f(t, v) =$$

$$\frac{\rho}{(2\,\pi T)^{3/2}} (\beta(t) + 1)^{3/2} \left(1 + \beta(t) \left(\frac{\beta(t) + 1}{2T} |v|^2 - \frac{3}{2} \right) \right) \mathrm{e}^{-\frac{\beta(t) + 1}{2T} |v|^2},$$

with

$$\beta(t) = \frac{\beta_0 \, \mathrm{e}^{-\alpha \rho \, t/2}}{1 + \beta_0 \, (1 - \mathrm{e}^{-\alpha \rho \, t/2})},$$

27

Table 5: Approximation error for the BKW initial condition

K	L	n	N_L	N_{GL}	$L_2(\mathbb{R}^3)$-Norm	CF
11	0	12	38	16	$9.77 \cdot 10^{-5}$	-
12	0	13	38	16	$2.00 \cdot 10^{-5}$	4.89
13	0	14	38	16	$2.95 \cdot 10^{-6}$	6.78
14	0	15	38	16	$2.66 \cdot 10^{-7}$	11.09

where β_0 denotes the initial value for the function β and α is defined as

$$\alpha = C_0 \pi \int_0^\pi b(\cos\theta) \sin^3\theta \, d\theta \,.$$

This solution is non-negative for

$$0 \leq \beta_0 \leq 2/3 \,.$$

The density ρ and the temperature T are two additional parameters. We will use the following setting for our tests

$$C_0 = \frac{1}{4\,\pi} \,, \ b(\cos\theta) = 1 \,, \ \alpha = 1/3 \,, \ \rho = 1 \,, \ T = 1 \,, \ \beta_0 = 2/3,$$

leading to the solution

$$f(t,v) = \frac{1}{(2\,\pi)^{3/2}} \left(\beta(t) + 1\right)^{3/2} \left(1 + \beta(t)\left(\frac{\beta(t)+1}{2}|v|^2 - \frac{3}{2}\right)\right) e^{-\frac{\beta(t)+1}{2}|v|^2} \,,$$

where

$$\beta(t) = \frac{2\,e^{-t/6}}{5 - 2\,e^{-t/6}} \,.$$

Initial condition

Since the BKW solution is an isotropic function, we change only the parameter K and let L be zero for all tests. This leads to a very low number of unknowns and to an extremely fast numerical solution of the Boltzmann equation taking only a few seconds. A stable spectral convergence starts with $K = 11$ and the results of the approximation of the initial condition are shown in Table 5 and in Figure 10. However, for these values no optical difference to the initial condition and to the final Maxwell distribution can be seen on a figure. Thus, we show the approximation of the initial condition and of the final Maxwell distribution for $K = 6$, $n = 7$ in Figure 9.

Relaxation of the moments

For the BKW solution, all physical moments remain constant in time and they are approximated with an accuracy of about $10^{-14} - 10^{-15}$ even for $n = 7$. Thus, we
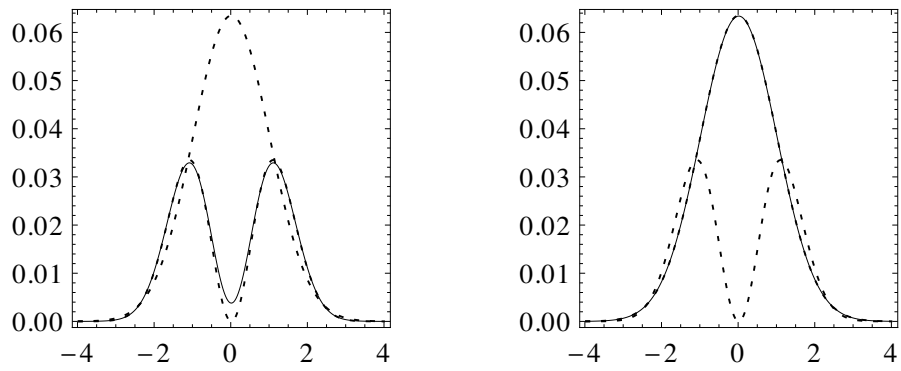
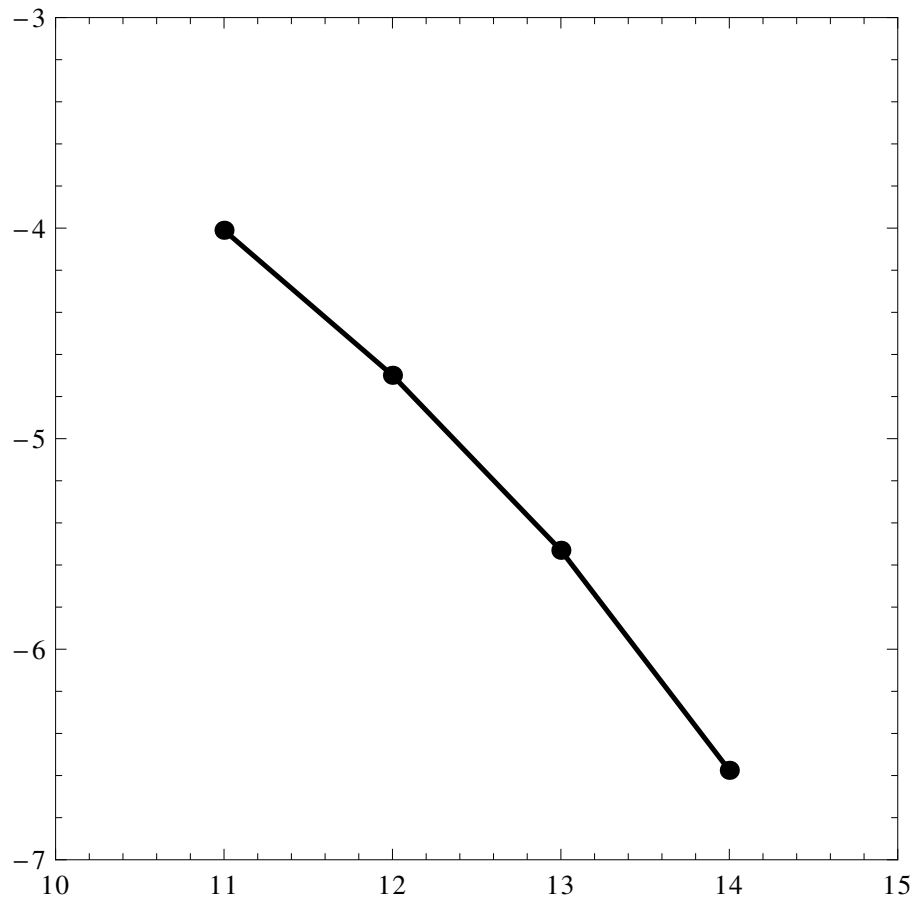Figure 9: Initial and final distributions for $n = 7$, BKW

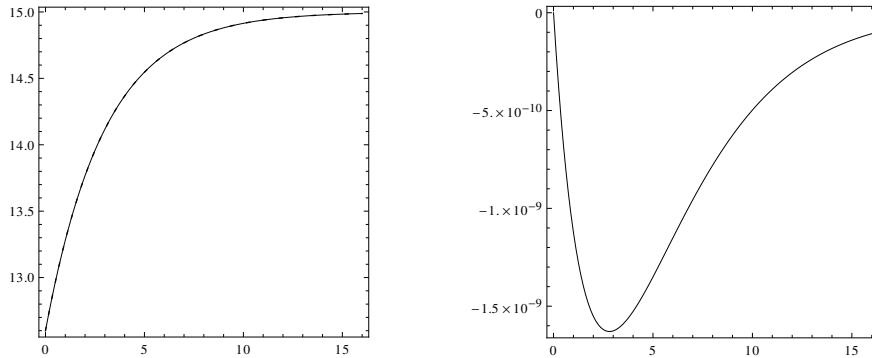Figure 10: $\log_{10}$ course of the $L_2(\mathbb{R}^3)$ error, BKW

Figure 11: Course of the functional $s(t)$, BKW

show only the course of the fourth moment $s(t)$ on the time interval $[0, 16]$ as well as the difference to the exact curve for $n = 7$ in Figure 11. The results are obtained with the Runge-Kutta method of the fourth order with $N_t = 128$ time steps.

5.3   Hard spheres

There is no analytic information about the exact solution for the case of hard spheres. Thus, we consider the above mixture of two Maxwell distributions as the initial condition and choose the solution obtained by the use of the stochastic particle method (see [42]) as a reference. We choose 8192 equally weighted particles and compute 8192 independent trajectories of the process on the time interval $[0, 4]$. Thus the accuracy of the stochastic solution should be of the order $10^{-3} - 10^{-4}$. For comparison, we take the curves obtained for $K = L = 4$, i.e. for $n = 125$ unknowns. For the time integration, the Runge-Kutta method of the fourth order with $N_t = 128$ time steps has been used. The dependence of the moment $M_{11}(t)$ on time is shown in Figure 12. The thick dashed line represents the stochastic reference solution on the left plot. The thin solid line is the Galerkin-Petrov solution. The right plot shows the difference between the curves. The accuracy is of the order 10^{-4}. The same data is shown for the fourth moment $s(t)$ in Figure 13. Here, the accuracy is of the order 10^{-3} and some oscillations of the stochastic solution are apparent. The computational time for the stochastic particle method on a single Intel i7 processor was about 10 minutes while the Galerkin-Petrov solution with precomputed collision matrices ($N_{GL} = 8$, $N_L = 50$) was obtained in 20 seconds. The computational time for the collision matrices was about 12 minutes, which is to the computation time of the stochastic solution. It seems, that the error is mostly due to the stochastic approximation, but to obtain an additional order of its accuracy, the computational effort must be increased 100-fold .
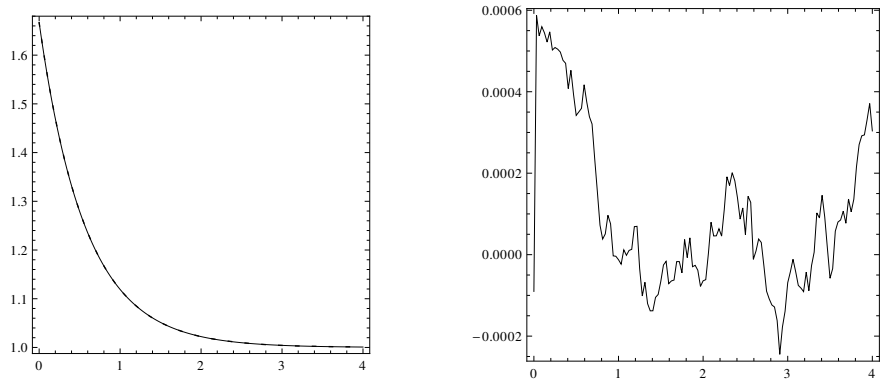
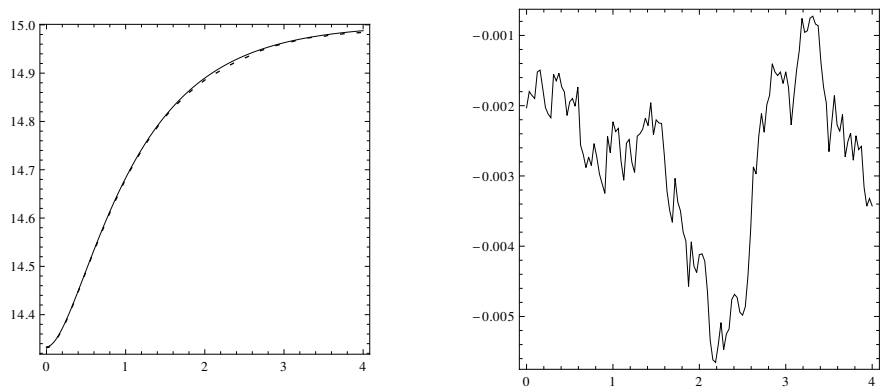Figure 12: Course of the functional $M_{11}(t)$, Hard Spheres

Figure 13: Course of the functional $s(t)$, Hard Spheres

6 Conclusions

In this paper we present a new deterministic numerical scheme for the classical spatially homogeneous Boltzmann equation. The scheme is based on a spectral Galerkin-Petrov scheme. The main features of the method are the following:

1. The method uses mutually orthonormal, globally defined basis functions derived from the normalised Maxwell distribution, the Laguerre polynomials and the spherical harmonics;

2. The system of test functions consists of globally defined low order polynomials;

3. Since the set of test functions contains all collision invariants, the method is automatically conservative, i.e. the numerical collision invariants remains constant up to the machine accuracy without any additional numerical effort;

4. The approximation quality of the method is spectral, i.e. there is an exponential convergence. However, this property holds only for infinitely smooth functions;

5. The main numerical work of the method is the initial computation of the collision matrices. However, once computed, these matrices can be used for different initial conditions, on different time intervals and for different time integration schemes. Then the computational procedure for the whole relaxation in time takes only seconds on a single processor;

6. Two classical numerical examples for the spatially homogeneous relaxation, namely mixture of two Maxwell distributions as an initial condition and the BKW solution were computed up to a very high accuracy with a low number of basis function of $10^1 - 10^3$;

7. The error due to the time integration dominated over the spectral error. The Runge-Kutta method of the fourth order was sufficient to equalise both errors;

8. For the hard spheres model, we've shown an excellent agreement of the results obtained by the new scheme with those obtained by a stochastic particle scheme.

A future work in this research area should certainly contain the following points:

1. Development of numerical integration quadratures for non-cutoff kernels B for an effective evaluation of the integrals (26), as mentioned in the end of Section 3;

2. Spatially homogeneous numerical tests to understand how far can the computations be done with the deviation of the temperature from its value equal to one and with the deviation from the zero mean velocity. This will help to formulate criteria for an enrichment of the system of the basis functions;

3. The method can be easily adapted for the inelastic Boltzmann equation with constant or even variable (relative velocity dependent) restitution coefficient. The main difference is in the term (26). However, since the tails of the distribution function of the inelastic Boltzmann equation exhibit an asymptotic different from the Maxwell distribution, the system of basis function should be modified as well;

4. The main goal is an application of the proposed approach to the spatially inhomogeneous Boltzmann equation. In this case the system (22) of ODE's will be transformed into the hyperbolic system

$$
\frac{\partial}{\partial t}\Big(M\underline{f}(t,x)\Big)_i + \mathrm{div}_x(F_i\underline{f}(t,x)) = \underline{f}(t,x)^\top Q_i\,\underline{f}(t,x)\,, \quad i = 1,\dots,n\,,
$$

where the flow matrices $F_i \in \mathbb{R}^{3\times n}$ have the entries

$$
F_i[m,j] = <v_m\varphi_j,\psi_i>\,, \quad m = 1,2,3\,,\ j = 1,\dots,n\,.
$$

for $i = 1,\dots,n$. These matrices can be easily precomputed and stored requiring much less memory than the collision matrices Q_i;

5. The proposed spatially inhomogeneous method can be especially efficient for very slow flows with a small deviation of the temperature from its mean value. Exactly for such flows, the application of the stochastic particle methods is problematic;

6. In spatially inhomogeneous flows, the situations occur where the distribution function becomes almost discontinuous. Thus, the system of basis functions should be enriched to account for this fact. The appropriate choice of functions for such enrichment is a topic for further research.

7. A rigorous proof of error estimates and the convergence to the Boltzmann-Maxwell equilibrium for the case of hard potentials with cut-off collision kernels is also a subject of an upcoming study.

7 Acknowledgement

References

[1] R. J. Alonso, I. M. Gamba, and S. H. Tharkabhushanam. Convergence and error estimates for the Lagrangian based conservative spectral method for Boltzmann equations. *Submitted for Publication*, 2016.

[2] V. Aristov. *Direct methods for solving the Boltzmann equation and study of nonequilibrium flows*, volume 60 of *Fluid Mechanics and its Applications*. Kluwer Academic Publishers, Dordrecht, 2001.

[3] H. Babovsky. Discrete kinetic models in the fluid dynamic limit. *Comput. Math. Appl.*, 67(2):256–271, 2014.

[4] H. Babovsky. Translation invariant kinetic models on integer lattices. In *AIP conference proceedings*, pages 640–647, Melville, NY, 2014.

[5] M. Bebendorf, A. Kühnemund, and S. Rjasanow. An equi-directional generalization of adaptive cross approximation for higher-order tensors. *Applied Numerical Mathematics*, 74:1–16, 2013.

[6] N. Bernhoff and A. Bobylev. Weak shock waves for the general discrete velocity model of the Boltzmann equation. *Commun. Math. Sci.*, 5(4):815–832, 2007.

[7] G. A. Bird. Monte Carlo simulation in an engineering context. *Progr. Astro. Aero*, 74 : 239–255, 1981.

[8] A. Bobylev and M. C. Vinerean. Construction and classification of discrete kinetic models without spurious invariants. *Riv. Mat. Univ. Parma (7)*, 7:1–80, 2007.

[9] A. V. Bobylev. Fourier transform method in the theory of the Boltzmann equation for Maxwell molecules. *Doklady Akad. Nauk SSSR*, 225 : 1041–1044, 1975.

[10] A. V. Bobylev, I. M. Gamba, and C. Zhang. On the rate of relaxation for the Landau kinetic equation and related models. *J. Statist. Phys.*, 2017.

[11] A. V. Bobylev, A. Palczewski, and J. Schneider. On approximation of the Boltzmann equation by discrete velocity models. *C.R. Acad. Sci. Paris*, 320 : 639–644, 1995.

[12] A. V. Bobylev and S. Rjasanow. Difference scheme for the Boltzmann equation based on Fast Fourier Transform. *Eur. J. Mech. B/Fluids*, 16(2) : 293–306, 1997.

[13] A. V. Bobylev and S. Rjasanow. Fast deterministic method of solving the Boltzmann equation for hard spheres. *Eur. J. Mech. B/Fluids*, 18(5) : 869–887, 1999.

[14] A. V. Bobylev and S. Rjasanow. Numerical solution of the Boltzmann equation using fully conservative difference scheme based on the Fast Fourier Transform. *Transport Theory Statist. Phys.*, 29(3-5): 289–310, 2000.

[15] R. Duduchava and S. Rjasanow. Mapping properties of the Boltzmann collision operator. *Integral Equations Operator Theory*, 52(1):61–84, 2005.

[16] A. Ya. Ènder and I. A. Ènder. Polynomial expansions for the isotropic Boltzmann equation and invariance of the collision integral with respect to the choice of basis functions. *Phys. Fluids*, 11(9):2720–2730, 1999.

[17] A. Ya. Ènder and I. A. Ènder. Properties of the collision integral in the axisymmetric Boltzmann equation. *Transport Theory Statist. Phys.*, 36(7):563–588, 2007.

[18] E. Fonn. *Approximation in Space and Velocity for Kinetic Transport Equations.* PhD thesis, ETH, Zürich, 2013.

[19] I. M. Gamba. Deterministic solvers for non-linear kinetic flows: A conservative spectral scheme for boltzmann type flows. In R. Abgrall and C-W. Shu, editors, *Handbook on numerical methods for hyperbolic problems*, chapter 15. Elsevier, 2017.

[20] I. M. Gamba and J. R. Haack. A conservative spectral method for the Boltzmann equation with anisotropic scattering and the grazing collisions limit. *J. Comput. Phys.*, 270:40–57, 2014.

[21] I. M. Gamba, J. R. Haack, C. D. Hauck, and J. Hu. A fast spectral method for the Boltzmann collision operator with general collision kernels. *SIAM Journal for Scientific Computing*, To appear, 2017.

[22] I. M. Gamba and S. H. Tharkabhushanam. Spectral-Lagrangian methods for collisional models of non-equilibrium statistical states. *J. Comput. Phys.*, 228(6):2012–2036, 2009.

[23] I. M. Gamba and S. H. Tharkabhushanam. Shock and boundary structure formation by spectral-Lagrangian methods for the inhomogeneous Boltzmann transport equation. *J. Comput. Math.*, 28(4):430–460, 2010.

[24] D. Goldstein, B. Sturtevant, and J. E. Broadwell. Investigation of the motion of discrete-velocity gases. In E.P. Muntz, D.P. Weaver, and D.H. Campbell, editors, *Rarefied Gas Dynamics: Theoretical and computational techniques*, pages 100–117. Progress in Astronomics and Aeronautics, 118, 1989.

[25] A. Heintz, P. Kowalczyk, and R. Grzhibovskis. Fast numerical method for the Boltzmann equation on non-uniform grids. *J. Comput. Phys.*, 227(13):6681–6695, 2008.

[26] I. Ibragimov and S. Rjasanow. Numerical solution of the Boltzmann equation on the uniform grid. *Computing*, 69(2):163–186, 2002.

[27] I. Ibragimov and S. Rjasanow. Three way decomposition for the Boltzmann equation. *J. Comp. Math.*, 27:184–195, 2009.

[28] G. Kitzler and J. Schöberl. Efficient spectral methods for the spatially homogeneous Boltzmann equation. Technical Report 13/2013, Institute for Analysis and Scientific Computing, Vienna University of Technology, Austria, 2013.

[29] S. Kosuge, K. Aoki, and S. Takata. Shock-wave structure for a binary gas mixture: Finite-difference analysis of the Boltzmann equation for hard-sphere molecules. *Eur. J. Mech., B/Fluids*, 20:87–, 2001.

[30] M. Krook and T. T. Wu. Exact solutions of Boltzmann equation. *Phys. Fluids*, 20(10):1589–1595, 1977.

[31] V. I. Lebedev. Quadratures on the sphere. *Ž. Vyčisl. Mat. i Mat. Fiz.*, 16(2):293–306, 539, 1976.

[32] V. I. Lebedev. Quadrature formulas for the sphere of 25th to 29th order accuracy. *Sibirsk. Mat. Ž.*, 18(1):132–142, 239, 1977.

[33] A. Munafo, J. R. Haack, I. M. Gamba, and T. E. Magin. A spectral-Lagrangian Boltzmann solver for a multi-energy level gas. *Jour. Comp. Phys.*, 264:152–176, 2014.

[34] A. Narayan and A. Klöckner. Deterministic Numerical Schemes for the Boltzmann Equation. ArXiv e-prints, 2009.

[35] T. Ohwada. Structure of normal shock waves: direct numerical analysis of the Boltzmann equation for hard-sphere molecules. *Phys. Fluids A*, 5(1):217–234, 1993.

[36] A. Palczewski and J. Schneider. Existence, stability, and convergence of solutions of discrete velocity models to the Boltzmann equation. *J. Statist. Phys.*, 91(1-2):307–326, 1998.

[37] V. A. Panferov and A. G. Heintz. A new consistent discrete-velocity model for the Boltzmann equation. *Math. Methods Appl. Sci.*, 25(7):571–593, 2002.

[38] L. Pareschi and B. Perthame. A Fourier spectral method for homogeneous Boltzmann equations. *Transport Theory Statist. Phys.*, 25 : 369–382, 1996.

[39] L. Pareschi and G. Russo. Numerical solution of the Boltzmann equation. I. Spectrally accurate approximation of the collision operator. *SIAM J. Numer. Anal.*, 37(4):1217–1245 (electronic), 2000.

[40] L. Pareschi and G. Russo. On the stability of spectral methods for the homogeneous Boltzmann equation. In *Proceedings of the Fifth International Workshop on Mathematical Aspects of Fluid and Plasma Dynamics (Maui, HI, 1998)*, volume 29, pages 431–447, 2000.

[41] T. Płatkowski and R. Illner. Discrete velocity models of the Boltzmann equation: a survey on the mathematical aspects of the theory. *SIAM Rev.*, 30(2):213–255, 1988.

[42] S. Rjasanow and W. Wagner. *Stochastic numerics for the Boltzmann equation.* Number 37 in Springer Series in Computational Mathematics. Springer, Berlin-Heidelberg-NewYork, 2005.

[43] F. Rogier and J. Schneider. A direct method for solving the Boltzmann equation. *Transport Theory Statist. Phys.*, 23(1-3) : 313–338, 1994.

[44] H. E. Salzer and R. Zucker. Table of the zeros and weight factors of the first fifteen Laguerre polynomials. *Bull. Amer. Math. Soc.*, 55:1004–1012, 1949.

[45] B. Shizgal. *Spectral methods in chemistry and physics.* Scientific Computation. Springer, Dordrecht, 2015. Applications to kinetic theory and quantum mechanics.

[46] W. Wagner. Approximation of the Boltzmann equation by discrete velocity models. *J. Statist. Phys.*, 78(5-6):1555–1570, 1995.

[47] C. Zhang. *On Studies of Deterministic Conservative Solvers for The Nonlinear Boltzmann and Landau Transport Equations.* PhD thesis, ICES, The University of Texas at Austin, 2014.

[48] C. Zhang and I. M. Gamba. A conservative scheme for vlasov poisson landau modeling collisional plasmas. *J. Comput. Physics,*, to appear, 2017.

[49] C. Zhang and I. M. Gamba. Spectral gap computations for linearized boltzmann operators. *submitted for publication*, 2017.